A Wind Tunnel Investigation of a Small-Scale Tiltrotor Model in Descending Flight

Anita I Abrego, Aerospace Engineer
aabrego@mail.arc.nasa.gov
NASA Ames Research Center
Moffett Field, CA

Kurtis R. Long, Aerospace Engineer
klong@mail.arc.nasa.gov
US Navy
Moffett Field, CA

Abstract

A small-scale tiltrotor model was tested in the 7- by 10-foot Wind Tunnel at NASA Ames Research Center, with the goal of better understanding Vortex Ring State (VRS) effects on tiltrotor aircraft. Test objectives were to obtain performance data of a tiltrotor model over a wide range of descent conditions, to explore the effects of sideslip at these descent conditions, and to investigate the validity of using a single-rotor with a physical image plane to simulate dual-rotor performance characteristics. The model consisted of a pair of 2-bladed teetering rotors with untwisted, 11.125-inch diameter, rectangular planform blades Model configuration variations included a dual-rotor, an isolated-rotor, and a single-rotor with a physical image plane Rotor performance data were obtained for the dual-rotor configuration operating over a wide range of descent and sideslip conditions Isolated-rotor and single-rotor with image plane configurations were tested over an abbreviated range of descent conditions. Results of this investigation are presented and show mean thrust reductions in the region of VRS for each model configuration In comparison with the dual-rotor configuration, the isolated-rotor and single-rotor with image plane configurations produced thrust results similar in trend but different in magnitude

Notation

C_T	Thrust coefficient, $T/\rho N_R(\Omega R)^2\pi R^2$
N_R	Number of rotors
R	Rotor radius, ft
T	Total model thrust, lb
V	Air velocity, ft/sec
V_{tip}	Rotor tip speed, ΩR, ft/sec
v_h	Equivalent hover induced velocity, $(T/2N_R\rho\pi R^2)^{1/2}$
α	Shaft angle, positive in descent , deg
α_G	Turntable angle, positive clockwise, deg
β	Model sideslip angle, deg
β_G	Sting pitch angle from horizontal, positive up, deg
θ	Rotor collective pitch angle, deg
ρ	Air density, slugs/ft^3
Ω	Rotor rotational speed, rad/sec

Introduction

Vortex Ring State (VRS) develops when a rotor's descent velocity approaches the induced wake velocity, causing the formation of a doughnut shaped vortex ring around the circumference of the rotor disk As VRS develops, the flow becomes very unsteady, causing a reduction in rotor thrust at constant collective blade pitch

The aerodynamic characteristics of helicopters operating in VRS have been studied for many years In the 1960's, two propellers were tested in vertical or near vertical descent, indicating a loss in thrust, as well as thrust oscillations, in the region of VRS (Ref 1) Researchers have also completed studies on both single and tandem rotor configurations operating in VRS conditions, each indicating thrust fluctuations in the region of VRS (Refs 2 and 3) More recently, a wind tunnel test was completed with the objective of studying VRS effects on tiltrotor aircraft (Ref. 4) In Ref 4, a single rotor operating in close proximity to a physical image plane was tested over a wide range of descent conditions, showing both mean thrust reductions and thrust oscillations initially developing at descent angles ranging from 30-deg to 40-deg However, there remained an incomplete understanding

Presented at the American Helicopter Society Aerodynamics, Acoustics, and Test and Evaluation Technical Specialists Meeting, San Francisco, CA, January 23-25, 2002

of the complicated aerodynamic environment associated with VRS, particularly for tiltrotor aircraft operating in descending flight conditions.

In February 2001, NASA Ames Research Center and the US Navy completed a wind tunnel experiment with the objective of gaining a better understanding of the aerodynamics of tiltrotor flight in descent. This experiment measured the loads experienced by a small-scale tiltrotor model in helicopter mode, operating at various states of descent and sideslip. A specific objective of this study was to further investigate the validity of using a single-rotor with image plane configuration to model a dual-rotor aerodynamic environment.

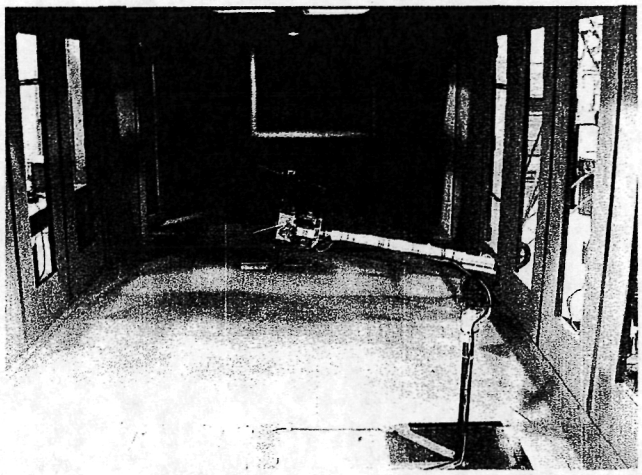

Figure 1. Tiltrotor Descent Aerodynamics test in the Ames 7- by 10-Foot Wind Tunnel.

Test Description

Installation

Figure 1 shows the test installation of a small-scale tiltrotor model in the 7- by 10-Foot Wind Tunnel at Ames Research Center. The model was located at the center of the test section to minimize wall effects. The model was attached to an extension arm in a sideward orientation, equivalent to a 90-deg roll. Model shaft angle-of-attack changes were provided by the wind tunnel turntable and sideslip, relative to the model longitudinal centerline, was achieved by rotating the extension arm upward about a horizontal axis. Because the pitch axis, or turntable axis, did not yaw with the model in sideslip, shaft angle-of-attack and sideslip changes were not independent. Therefore, true shaft angle-of-attack and sideslip angle for the model were computed from the geometric pitch (α_G) and yaw (β_G) angles as follows:

$$\alpha = \tan^{-1}(\tan\alpha_G / \cos\beta_G) \qquad (1)$$

$$\beta = \sin^{-1}(\cos\alpha_G \sin\beta_G) \qquad (2)$$

Isolated-rotor testing was achieved by removing the left-hand rotor blade set. A 30-inch diameter image plane was installed horizontally below the model, 1.15R from the center of the rotor for the single-rotor with image plane test configuration (Fig. 2). Tufts were used to visualize airflow along the image plane. This approach of locating the image plane outboard of the model, rather than at the model centerline, resulted in the image plane being located on the advancing side of the rotor instead of the retreating side. Therefore, this method did not properly represent the relationship between the rotor and the aircraft centerline, which is on the retreating side of current tiltrotor aircraft rotors. It is not known whether this difference was significant.

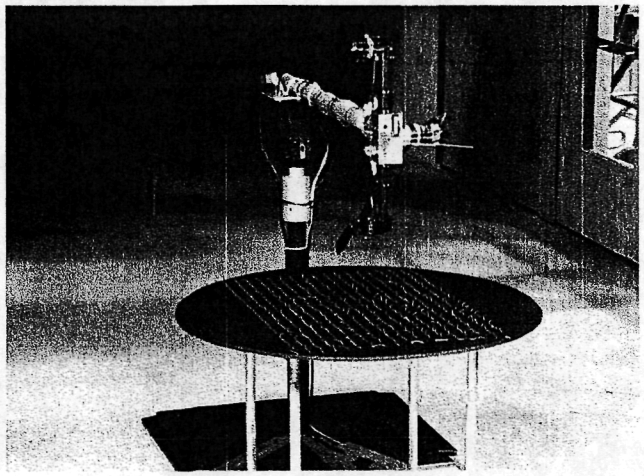

Figure 2. Single-rotor with image plane configuration.

Model

The tiltrotor model was constructed using off-the-shelf radio-controlled (R/C) model helicopter parts. Figure 3 shows the dual-rotor model configuration with 2-bladed, untwisted, teetering rotors. The rotor separation distance was 2.55R and the rotors were configured such as a conventional tiltrotor with outboard advancing blades. Model parameters are provided in Table 1.

Commercially available hobbyist radio control, transmitter, receiver, speed control and rpm governor units were used to remotely command rotor rpm and collective pitch. A 700W brushed electric motor provided power to the model.

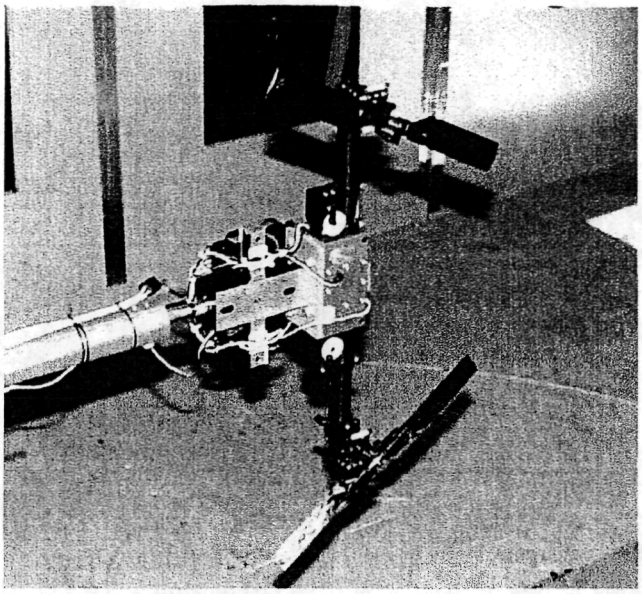

Figure 3. Dual-rotor configuration of tiltrotor model.

Table 1. Model parameters.

Parameter	Value
Diameter	11.125 in
Chord	1.13 in
Twist	0 deg
Thrust-weighted solidity	0.13
Rotor separation distance	2.55R
Lock number	0.183

Test Conditions

Dual-rotor, isolated-rotor, and single-rotor with image plane performance data were acquired over the test conditions shown in Table 2. Rotor speed was held constant at 5000 rpm, producing a tip speed of 243 ft/sec. Variable test parameters for each model configuration included advance ratio (V/V_{tip}), collective blade pitch (θ), and model shaft angle-of-attack (α). Sideslip angle (β), was introduced for the dual-rotor configuration only. There was no measure of blade flapping, therefore descent angle is used within this paper when referring to shaft angle-of-attack.

For each collective blade pitch, descent angle was varied from 0 to 90 deg. Advance ratios ranging from 0 to 0.13 were tested for the dual-rotor configuration. The dual-rotor configuration testing also included descent angle and collective pitch variations for sideslip angles ranging from 0 to 30 deg. Isolated-rotor and single-rotor with image plane runs was performed over a smaller range of advance ratios.

Table 2. Test conditions

Parameter	Dual-Rotor	Isolated-rotor, Single-rotor with Image Plane
V_{tip} (ft/sec)	243	243
V/V_{tip}	0 to 0.13	0, 0.06, 0.08
θ (deg)	0, 3, 6, 9, 12, 15, 18, 20.4	0, 3, 6, 9, 12, 15, 18, 20.4
α_G (deg)	0, 10, 20, 25, 30, 35, 40, 45, 50, 55, 60, 70, 80, 90	0, 10, 20, 25, 30, 35, 40, 45, 50, 55, 60, 70, 80, 90
β_G (deg)	0 to 30	-

Data Acquisition and Instrumentation

Model balance data were low-pass filtered at 100 Hz and acquired at 1024 samples per second per channel. Data were recorded at each test condition for an 8-second duration, producing time history records of 8192 samples for each record. Time history records were averaged to produce mean data.

A 6-component internal balance was used to measure model forces and moments. Mean thrust was used to calculate the vehicle thrust coefficient. A vane anemometer, with a range of 1 to 130 ft/sec, was installed upstream of the model to measure air velocity in the wind-tunnel test section.

Results and Discussion

The effects of VRS on mean rotor thrust will be shown for the dual-rotor configuration for the full range of descent angles. Sideslip effects on dual-rotor mean rotor thrust will be shown. Isolated-rotor, single-rotor with image plane, and dual-rotor thrust results will be presented and discussed.

Mean Rotor Thrust and Moments

Using Ref. 4 as a guide, descent angle sweeps were focussed on the 0.08 and 0.10 advance ratio conditions. In addition, descent angle sweeps were also performed at 12 and 18-deg collective pitch for an advance ratio of 0.06. Figure 4 shows the dual-rotor thrust variation as a function of descent angle, for constant advance ratio and collective pitch. Initially, thrust increases as a function of descent angle. Depending on advance ratio and collective pitch, the thrust begins to decrease with increasing descent angle between 10 to 40 deg. The 0.06 and 0.08 advance ratio curves, show an initial thrust reduction between 20 and 30 deg. The 0.10 advance ratio curves reveal thrust reductions as early as 10 deg for higher collective pitch curves, as well as the lower collective pitch curves

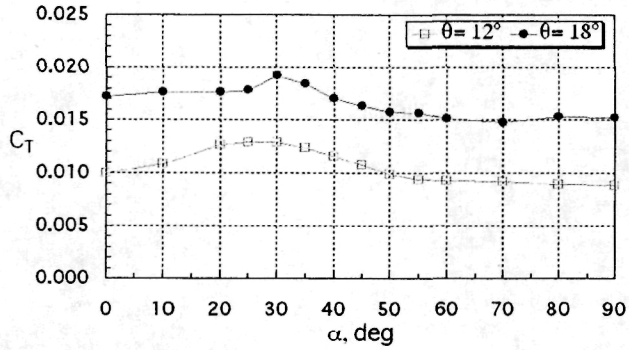

a) V/V_{tip} = 0.06

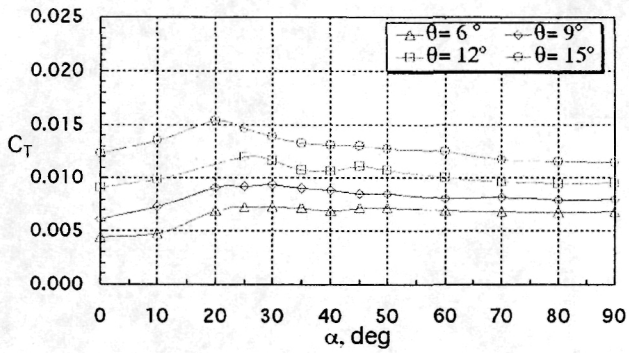

b) V/V_{tip} = 0.08

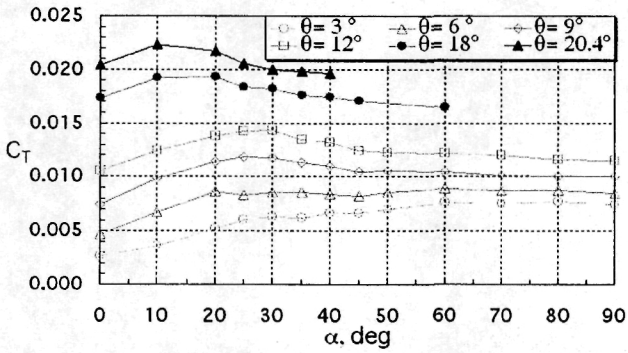

c) V/V_{tip} = 0.10

Figure 4. Variation of mean vehicle thrust coefficient with descent angle.

gradually increasing with descent angle and then leveling off. The thrust reductions occurring between descent angles of 10-40 deg are consistent with general VRS characteristics.

An additional method used to investigate VRS effects is to examine the effective lift curve slope (Ref. 4). Figure 5 shows the mean vehicle thrust coefficient versus collective pitch at constant descent angles for advance ratios of 0.08 and 0.10. The slopes of all the curves are positive; indicating higher thrust is always achieved by increasing collective pitch. A reduction in the lift curve slope occurs at descent angles consistent with the initial thrust reductions seen in Fig. 4. Figure 5a, at 0.08 advance ratio, reveals a slope reduction between the 25 and 30 deg descent angle curves. Similarly, Fig. 5b reveals a decrease in slope occurring between descent angles of 30 and 40 deg for an advance ratio of 0.10. This decrease in the rotor's effective lift curve slope is attributed to the reduction in thrust caused by VRS.

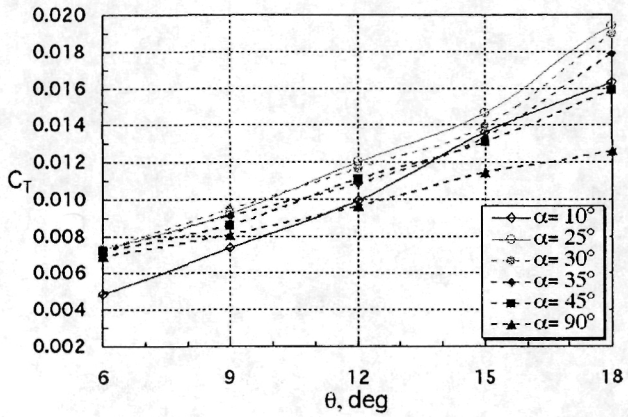

a) V/V_{tip} = 0.08

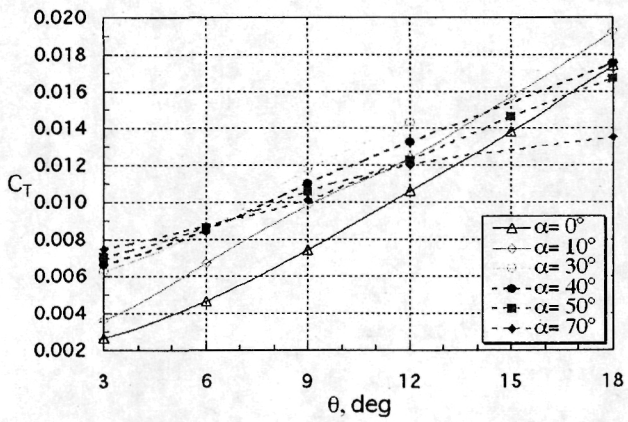

b) V/V_{tip} = 0.10

Fig. 5. Variation of thrust coefficient with collective pitch, no sideslip, dual-rotor configuration.

Data from Fig. 5 were cross-plotted to illustrate the collective pitch required to maintain constant thrust (Fig. 6). Initially, collective pitch decreases as descent angle increases. Again, at descent conditions earlier identified as regions of VRS, an increase in collective pitch is required to maintain constant thrust. Figure 6a shows an increase in collective pitch at descent angles between 20 and 40 deg, for the 0.08 advance ratio case. Similarly, at 0.10 advance ratio, an increase in collective pitch is needed

beginning at descent angles beginning between 20 and 30 deg This increase in the required collective pitch is a result of VRS thrust reductions and a reduction in the rotor's effective lift curve slope

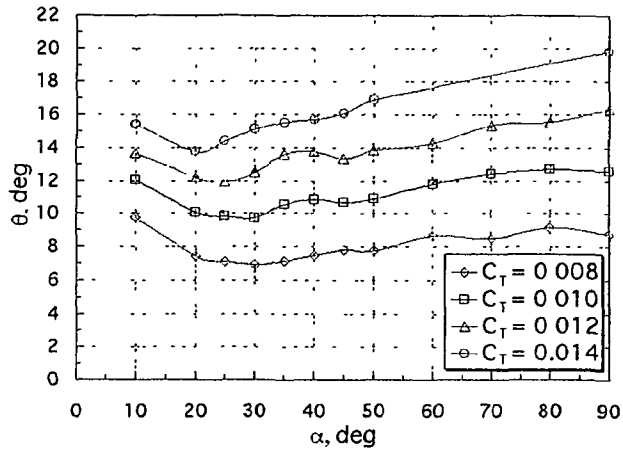

a) V/V_{tip} = **0.08**

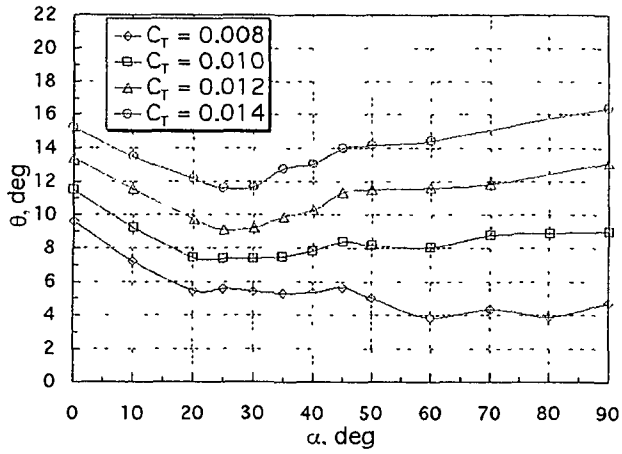

b) V/V_{tip} = **0.10**

Fig. 6. Collective pitch required to maintain constant thrust coefficient, no sideslip, dual-rotor configuration.

Effect of Sideslip on Mean Rotor Thrust

Data were acquired for the dual-rotor configuration, at sideslip angles ranging from 0 to 30 deg The effects of sideslip angle on mean rotor thrust are shown in Figure 7, where thrust coefficient is plotted versus collective pitch, at 30-deg descent angle Mean rotor thrust does not appear to be significantly affected by sideslip angles up to 13 deg at this descent condition, although additional testing should be performed to further investigate sideslip effects for a full range of sideslip and descent conditions

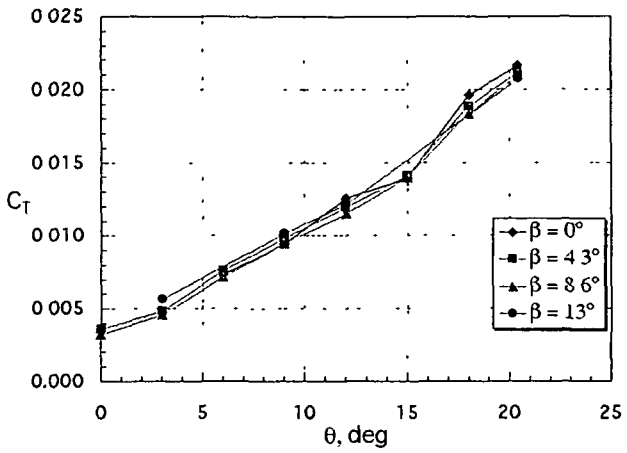

Figure 7. Effect of sideslip on mean vehicle thrust coefficient, dual-rotor configuration, V/V_{tip} = 0.08, α = 30 deg.

Isolated-rotor, Single-rotor with Image Plane, and Dual-rotor Comparison

Isolated-rotor and single-rotor with image plane data were acquired at 12 and 18 deg collective pitch for 0.06 and 0.08 advance ratios. Figure 8 shows mean rotor thrust, normalized by the mean thrust coefficient at 0-deg descent angle, for θ = 12 deg and V/V_{tip} = 0 08 The isolated-rotor

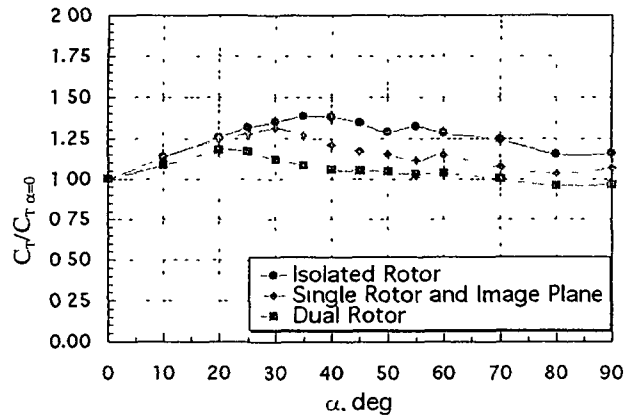

Fig. 8. Effect of image plane on mean thrust coefficient, V/V_{tip} = 0.08, θ = 12 deg.

configuration shows a greater increase in thrust with increasing descent angle, and a reduction in thrust beginning between 35 and 40-deg descent angle The single-rotor with image plane shows a similar increase in thrust, with a reduction in thrust beginning at a descent angle of 30 deg The dual-rotor configuration shows a much smaller increase in thrust with increasing descent angle and a thrust reduction beginning at an earlier descent angle of 20 deg The shallow decrease in thrust for the isolated-rotor case, as compared to the single rotor with image plane, agrees with the thrust versus descent angle

results reported in Ref. 4. Results from this test imply the dual-rotor configuration produces an even greater reduction in thrust

The descent angle at which the thrust begins to decrease due to VRS appears to depend on model configuration The single-rotor with image plane follows the general characteristics of a dual-rotor in the region of VRS, but does not properly characterize the descent angle at which the thrust reduction begins Further research should be conducted to determine the specific causes of the differences between the dual-rotor and the single-rotor with image plane results

Conclusions

An experimental investigation of a small-scale tiltrotor model was completed to study the Vortex Ring State (VRS) effects for three model configurations: a dual-rotor, an isolated-rotor, and a single-rotor with image plane configuration

The findings from this research effort are as follows

1 All three model configurations resulted in significant VRS induced thrust reductions beginning between descent angles of 10 to 40 deg.

2 A reduction in the dual-rotor lift-curve slope was evident between descent angles of 20 to 40 deg.

3 VRS effects on average thrust were not detected for the limited amount of sideslip conditions tested Descent angle and freestream velocity appear to have a greater influence on tiltrotor thrust characteristics in VRS conditions

4 The dual-rotor model configuration produced thrust results which were significantly different than the single-rotor with image plane, suggesting the single-rotor and image plane may not properly capture the aerodynamic nature of a dual-rotor vehicle.

Recommendations for future research are as follows.

1. A model which better represents the physical characteristics of a tiltrotor aircraft should be tested in VRS conditions Specific recommendations for model improvements include using three-bladed rotors, twisted blades, a tiltrotor fuselage and wings Additional research should be performed to further investigate the effects of model scale

2 Additional dual-rotor configuration testing is necessary to better understand the VRS effects on a tiltrotor In addition to the total vehicle force and moment measurements, individual rotor thrust and torque should be measured on a dual-rotor configuration

3 Additional single-rotor with image plane and dual- rotor comparison testing should be performed. The image plane of the single rotor should be located on the retreating side of the rotor.

4. A more complete sideslip investigation is needed to fully understand the combined sideslip and descent angle effects on VRS

Acknowledgements

The authors wish to recognize the invaluable technical and experimental support provided by several members of the Rotorcraft Aeromechanics Branch of the Army/NASA Rotorcraft Division and the U.S. Army Aeroflightdynamics Directorate Experimental Support Team at NASA Ames Research Center. Specifically, the authors wish to thank Perry Kavros for his expertise in R/C rotor models and Mark Betzina for providing advice and guidance during both the experimental and analytical phases of this test.

References

1) Yaggy, P. and Mort, K., "Wind-Tunnel Tests of Two VTOL Propellers in Descent," NASA TN D-1766, March 1963.
2) Washizu, K , Azuma, A , Koo, J , and Oka, T , "Experiments on a Model Helicopter Rotor Operating in the Vortex Ring State," *Journal of Aircraft*, Vol 3, No 3, May-June 1966.
3) Washizu, K , Azuma, A., Koo, J , and Oka, T "Experimental Study on the Unsteady Aerodynamics of a Tandem Rotor Operating in the Vortex Ring State," American Helicopter Society 22nd Annual Forum, Washington, DC, May 1966
4) Betzina, M., "Tiltrotor Descent Aerodynamics A Small-Scale Experimental Investigation of Vortex Ring State," American Helicopter Society 57th Annual Forum, Washington, DC, May 2001